A simple assay to probe disease-associated enzyme activity using glycosaminoglycan-assisted synthesized gold nanoparticles†

Zhihui Ban,*‡ Carlos J. Bosques‡ and Ram Sasisekharan*

Received 30th July 2008, Accepted 6th October 2008
First published as an Advance Article on the web 17th October 2008
DOI: 10.1039/b813210k

A simple assay to probe disease-associated enzyme activity using glycosaminoglycan-assisted synthesized gold nanoparticles is reported.

Glycosaminoglycans (GAGs), a common class of naturally encountered polysaccharides, have emerged as key players in a vast number of important biological functions such as angiogenesis, cell death, viral infection, tumor growth, *etc.*[1,2] More recently, GAG-modifying enzymes have also been directly associated with the progression of several diseases such as cancer. For example, increased activity of heparanases has been described as a major hallmark in the progression of multiple myeloma and the activity of these enzymes in the plasma of myeloma patients has been proposed as a surrogate to diagnose the disease.[3] Most current methods used to measure the activity of polysaccharide-degrading enzymes are very difficult to employ directly in biological environments (such as in the presence of cellular components or body fluids).[2] Given the important involvement of heparanases in cancer, it is important to design new methods that facilitate monitoring their activity.

Nanotechnology is becoming an increasingly recognized field as it starts to generate novel avenues to monitor and treat diseases. In particular, gold nanoparticles (GNPs) have received significant attention for biosensing applications based on their exceptional optical and electronic properties.[4,5] Although GNPs have been functionalized with proteins and DNA during the last 20 years, it is only recently that carbohydrates have started to be used in combination with gold nanoparticles.[6–13] However most of these studies have not employed polysaccharides.

Herein, we describe the template-assisted synthesis of GNPs with biologically-active glycosaminoglycans and illustrate the potential of these scaffolds to easily monitor disease-associated enzyme activity. As an example, we have generated heparan sulfate-coated GNPs which serve as useful scaffolds to monitor the activity of the myeloma-associated enzyme heparanase. To the best of our knowledge, the glycosaminoglycan-assisted aqueous preparation of gold nanoparticles has not been reported before. Specifically, the cleavage of the polysaccharide chains by the enzyme causes the aggregation of the GNPs which is accompanied by a red shift in the absorbance spectra. One important advantage of this assay is that alterations to the spectra are in a range that is very sensitive to the human eye (between 500 nm and 600 nm) which allows monitoring of the reaction visually. Also, this region of the spectrum is more transparent to the cellular environment, and therefore facilitates the activity-based profiling of polysaccharide-degrading enzymes directly in biological environments; something difficult to achieve with current available methods. Therefore, given the proven link between heparanase's activity and myeloma progression and the lack of simple assays to monitor heparanase activity, these scaffolds could potentially be used for myeloma diagnostics applications.

A drawback of glycosaminoglycans is their propensity for degradation (i.e. desulfation) during manipulation under harsh conditions and their limited reactive groups for derivatization. Therefore, in the generation of glycosaminoglycan-derived GNPs, we were interested in using a mild approach to limit the degradation of the polysaccharide as well as a method that would not only rely on reductive amination chemistry with the reducing end of the polysaccharide. After trying several conditions, we interestingly found that by mixing glycosaminoglycans in a specific sequence with metallic precursors in aqueous conditions, we were able to efficiently generate soluble biologically-active nanoparticles. For example, in a typical synthesis of heparan sulfate-GNPs, the gold precursor ($HAuCl_4$) is first mixed with the heparan sulfate in water followed by the addition of a trisodium citrate solution ($Na_3C_6H_5O_7$) and incubation at 60 °C for one hour. The resulting purple solution is then centrifuged to separate the unbound polysaccharide from the coated GNPs. As shown in Fig. 1, the preparation of the soluble gold nanoparticles seems to be assisted by the polysaccharide as their successful generation is dependent on the interaction of the gold precursor with the polysaccharide prior to the reaction with the trisodium citrate. That is, the soluble nanoparticles did not form under these conditions when the polysaccharide was added after the trisodium citrate or was not added at all. Standard methods usually generate

Fig. 1 Glycosaminoglycan-assisted synthesis of soluble GNPs. (A) Product of the reaction between the precursors where $HAuCl_4$ is mixed with $Na_3C_6H_5O_7$ in the absence of the polysaccharide. (B) Product when $HAuCl_4$ is mixed with $Na_3C_6H_5O_7$ followed by the addition of the polysaccharide. (C) Product when $HAuCl_4$ is first mixed with heparan sulfate followed by the addition of the trisodium citrate. GNP concentration is 51.2 μg/ml.

Department of Biological Engineering, Harvard-MIT Division of Health Science and Technology, Koch Institute for Integrative Cancer Research, Massachusetts Institute of Technology, 15-561, 77 Massachusetts Avenue, Cambridge, Massachusetts 02139, USA. E-mail: zban@mail.rochester.edu, rams@mit.edu

† Electronic supplementary information (ESI) available: Figure showing the effects of different control samples on the photophysical properties of the heparan sulfate-GNPs and TEM images of heparan sulfate-GNPs before and after treatment with enzyme. See DOI: 10.1039/b813210k

‡ These authors contributed equally to this work.

15 to 16 nm diameter gold nanoparticles[14,15] while the average diameter of our heparan sulfate-GNPs was determined to be 20 ± 5 nm *via* transmission electron microscopy (TEM). Although not significantly different, the somewhat "larger" size of our GNPs could potentially be due to the assistance of the polysaccharides during the reaction, which facilitates the process allowing the particles to be formed at lower temperatures and can apparently have an effect on the final size. In addition to the simplicity of this method, another major advantage of this approach over standard protocols[14,15] is that the lower temperature required to generate the particles can help preserve the stability of the glycosaminoglycans. These heparan sulfate-GNPs can be incubated in water at 4 °C for at least 2 weeks without apparent degradation. This approach has also been successfully applied to the preparation of other nanoparticles (e.g. CdS and PbS). This will be discussed in a separate report.

The polysaccharide-GNPs were then tested as substrates for polysaccharide degrading enzymes to evaluate their integrity as well as their potential as scaffolds to measure disease-associated enzyme activity. We first evaluated the response of the heparan sulfate-GNPs when exposed to heparinase in a simple buffer system. For this, 2 μL of enzyme (0.7 μg/μl heparinase III) was added to a cuvette containing a 1.5 ml polysaccharide-GNPs solution (GNPs: 51.2 μg/ml) and 1.5 ml of PBS buffer (without calcium chloride or magnesium chloride) pH 7.4 at 35 °C. The absorption spectrum between 400 and 800 nm was recorded as well as the absorption maxima as a function of time (Fig. 2). As observed in Fig. 2, treatment of the GNPs with the enzyme is accompanied by a large red shift in the visible spectrum from 542 nm to 567 nm that can be easily monitored with the naked eye (purple to blue). Additionally, increasing amounts of enzyme caused increased red shifting of the maxima peak. However, these changes to the absorbance spectra of the GNPs were not observed when the heparan sulfate-GNPs were exposed to BSA and human serum or plasma, which contains numerous proteins, but no enzyme added (see ESI† Fig. S1 for effects of different control samples on the photophysical properties of the heparan sulfate gold nanoparticles). This effect also seems to be dependent on the amounts of heparinase enzyme added to the GNP as a proportional increase in the 630 nm absorbance is obtained with the addition of heparinase (Fig. 3). The absorbances at 630 nm

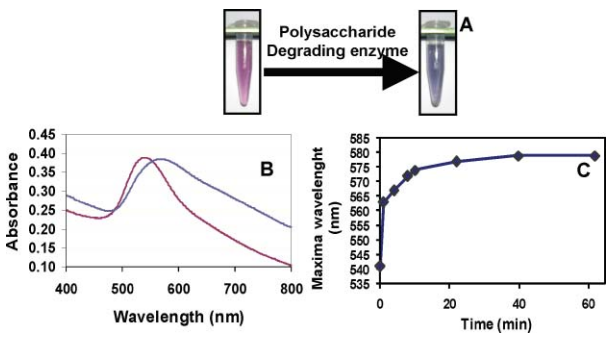

Fig. 2 Photophysical alterations to heparan sulfate-GNPs (25.6 μg/ml) upon treatment with 1.4 μg Heparinase III. Visible inspection (A) and absorbance spectra (B) of the solution before (purple) and after (blue) treatment with heparinase III. (C) Change in absorbance maxima as a function of enzyme treatment time.

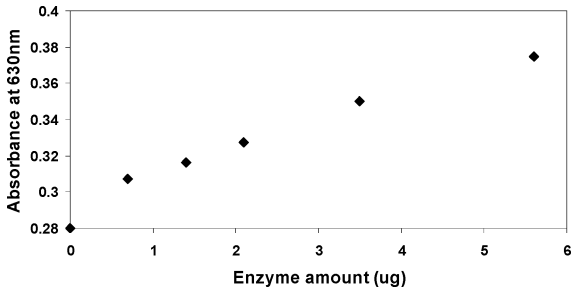

Fig. 3 Changes in the absorbance at 630 nm of the heparan sulfate-GNP as a function of heparinase amounts measured 8 minutes after enzyme addition. (25.6 g/ml GNPs, PBS buffer, pH 7.4 at 35 °C.)

were measured 8 minutes after addition of the enzyme to the same amount of GNP sample.

The light-absorptive and scattering properties of GNPs depend on the particle's size, aggregation state, shape, environment, and dielectric properties. Using transmission electron microscopy (TEM), we then confirmed the change in aggregation state of the particles upon the treatment with the enzyme. As illustrated in Fig. 4, before enzyme treatment the GNPs are well dispersed but they clustered together in an aggregate after the enzyme treatment (see also ESI† Fig. S2, which shows a different magnification of the TEM image in Fig. 4). Based on the above experiments, the agglutination is mainly due to the degradation of glycosaminoglycans on the surface of the nanoparticles. Fig. 4 also shows a schematic representation of the reaction which explains the observed biophysical responses.

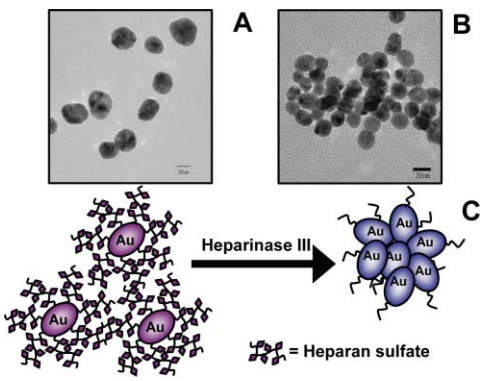

Fig. 4 TEM of heparan sulfate-GNPs (25.6 μg/ml) before (A) and after (B) treatment with 1.4 μg heparinase III. (C) Schematic representation of the aggregation of the GNPs upon enzyme treatment. Bar scale = 20 nm.

Lyase activity is usually measured by monitoring the 232 nm absorbance due to formation of the α, β-unsaturated uronides.[16,17] This measurement is usually performed in simple buffer systems to eliminate backgrounds since most biological species can easily interfere with the absorbance at 232 nm. Therefore, the analysis of enzyme activity with this method in the presence of more complex samples (such as biological fluids) is very challenging. To further demonstrate the use of our method, the assay was also performed directly on serum and plasma-containing samples (Fig. 5). For each sample, 1 ml of serum or plasma was added to a solution containing 1.5 ml of 51.2 μg/ml heparin sulfate-GNP in water and 0.4 ml of PBS buffer pH 7.4, and the final solution was spiked with 2 μl of enzyme (0.7 μg/μl heparinase III). The spectra were

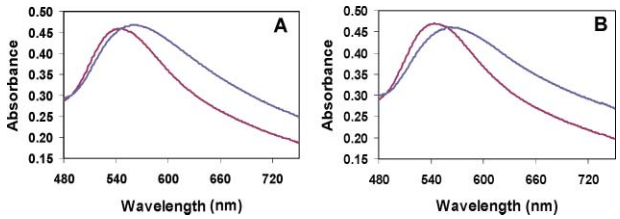

Fig. 5 Photophysical alterations to heparan sulfate-GNPs (26.4 μg/ml) before (purple) and after (blue) exposure to 1.4 μg heparinase III in serum (A) and plasma (B).

measured after 15 minutes. Red shifts from 542 nm to 558 nm and from 542 nm shift to 561 nm were observed for serum and plasma respectively. The smaller red shifts observed in this case (in comparison with the 25 nm red shift observed in buffer alone) could presumably be due to the negative electrostatic repulsions from plasma and serum.[18] However, the red shift is significant enough to monitor the enzyme activity.

In summary, we have described a simple approach for the aqueous preparation of complex polysaccharide-GNPs where the polysaccharides assist in the formation of the particles. These polysaccharide-GNPs were used for testing the activity of polysaccharide-degrading enzymes, *e.g.* heparinase III. As the activities of many polysaccharide-degrading enzymes are directly associated with many pathophysiological alterations in humans—such as tumor progression, neurological disorders and viral and bacterial infections—this method has the potential to become valuable for a wide variety of applications such as diagnostics, tissue-specific or site-specific profiling, monitoring of therapeutic efficacy, *etc.* Additionally, this method can be extended to other nanoparticles, such as quantum dots (PbS or CdS), magnetic nanoparticles and other materials, and some results have already been obtained in our lab. Therefore, this concept of using polysaccharide-coated nanoparticles to detect polysaccharide-modifying enzymes may have broad applicability for assessing enzyme biomarkers in many biological processes and disease pathologies.

Experimental Section

Materials

All chemicals were acquired from Sigma unless otherwise stated. Human serum was acquired from Biomeda.

GNP synthesis

For the synthesis of heparan sulfate-GNPs, we first mix 5.8 mg (0.013 mmol) of $HAuCl_4 \cdot 3H_2O$ with 4 mg of heparan sulfate I in 50 ml deionized water. After heating at 60 °C for 15 minutes, 1 ml of aqueous trisodium citrate solution ($Na_3C_6H_5O_7 \cdot 2H_2O$, 1%w/v) is added to the solution and kept at 60 °C for 60 minutes with continued stirring. The solution is then allowed to cool to room temperature. This generates a purple clear solution that is finally centrifuged and the supernatant is removed to separate the unbound polysaccharide from the coated GNPs.

UV and TEM

The optical absorption spectra of all samples were recorded with a DU 800 dual-beam Beckman Coulter spectrophotometer, using 1 cm path length quartz cuvettes. TEM images were obtained on a JEOL model 2011 that was operated at 200 kV. The samples for TEM analysis were prepared by evaporation of droplets placed on Formvar-carbon TEM grids.

Acknowledgements

This work was supported by the National Institutes of Health Grant T32-ES007020 (CB) and GM57073 (RS).

References

1 R. Sasisekharan, Z. Shriver, G. Venkataraman and U. Narayanasami, *Nat Rev Cancer*, 2002, **2**, 521–528.
2 T. Kudo, H. Nakagawa, M. Takahashi, J. Hamaguchi, N. Kamiyama, H. Yokoo, K. Nakanishi, T. Nakagawa, T. Kamiyama, K. Deguchi, S. Nishimura and S. Todo, *Molecular Cancer*, 2007, **6**, 32–41.
3 T. Kelly, H. Q. Miao, Y. Yang, E. Navarro, P. Kussie and Y. Huang, *et al.*, *Cancer Res*, 2003, **63**, 8749–8756.
4 J. M. Wessels, H. G. Nothofer, W. E. Ford, F. von Wrochem, F. Scholz and T. Vossmeyer, *et al.*, *J Am Chem Soc*, 2004, **126**, 3349–3356.
5 J. S. Hurst, M. S. Han, A. K. R. Lytton-Jean and C. A. Mirkin, *Anal. Chem.*, 2007, **79**, 7201–7205.
6 J. M. de La Fuente, A. G. Barrientos, T. C. Rojas, J. Rojo, J. Canada and A. Fernandez, *et al.*, *Angew Chem Int Ed Engl*, 2001, **40**, 2257–2261.
7 C. L. Schofield, A. H. Haines, R. A. Field and D. A. Russell, *Langmuir*, 2006, **22**(15), 6707–6711.
8 A. J. Reynolds, A. H. Haines and D. A. Russell, *Langmuir*, 2006, **22**(3), 1156–1163.
9 K. M. Halkes, S. Carvalhode, E. C. Adriana, P. Maliaars, G. J. Gerwig and J. P. Kamerling, *European Journal of Organic Chemistry*, 2005, **17**, 3650–3659.
10 S. Carvalho, de, H. Adriana, M. Koen, J. D. Meeldijk, A. J. Verkleij, J. F. G. Vliegenthart and J. P. Kamerling, *ChemBioChem*, 2005, **6**(5), 828–831.
11 J. Rojo, V. Diaz, J. M. De, la Fuente, I. Segura, A. G. Barrientos, H. H. Riese, A. Bernad and S. Penades, *ChemBioChem*, 2004, **5**(3), 291–297.
12 J. M. de la Fuente and S. Penades, *Biochimica et Biophysica Acta*, 2006, **1760**, 636–651.
13 M. A. Skidmore, S. J. Patey, N. T. K. Thanh, D. G. Fernig, J. E. Turnbull and E. A. Yates, *Chem. Commun.*, 2004, 2700–2701.
14 J. Turkevich, P. C. Stevenson and J. Hiller, *Discuss. Faraday Soc.*, 1951, **11**, 55–75.
15 G. Frens, *Nat. Phys. Sci.*, 1973, **241**, 20–22.
16 H. Bernstein, V. C. Yang, C. L. Cooney and R. Langer, *Methods Enzymol.*, 1988, **137**, 515–529.
17 R. Sasisekharan, M. Bulmer, K. W. Moremen, C. L. Cooney and R. Langer, *Proc. Natu. Acad. Sci. USA*, 1993, **90**, 3660–3664.
18 J. J. Green, J. Shi, E. Chiu, E. S. Leshchiner, R. Langer and D. G. Anderson, *Bioconjug Chem*, 2006, **17**, 1162–1169.

